Adsorption of sulfamonomethoxine antibiotics to cucurbit[6]uril-anchored silica gel: effect of aqueous solution chemistry

Tao Jin[a,b], Yun Liu[a,*], Yuan-hua Dong[a], De-qiang Chen[b], Hong-tao Qiao[a]

[a]*Key Laboratory of Soil Environment and Pollution Remediation, Institute of Soil Science, Chinese Academy of Sciences, Nanjing 210008, P.R. China, Tel. +86 25 86881370; Fax: +86 25 86881000; emails: 267286589@qq.com (T. Jin), yliu@issas.ac.cn (Y. Liu), yhdong@issas.ac.cn (Y.-h. Dong), 469494248@qq.com (H.-t. Qiao)*
[b]*Key Laboratory of Integrated Regulation and Resource Development on Shallow Lakes of Ministry of Education, Hohai University, Nanjing 210098, P.R. China, email: hjycdq@hhu.edu.cn (D.-q. Chen)*

ABSTRACT

Cucurbit[6]uril-anchored silica gel (ACB[6]-SG) was used to adsorb sulfamonomethoxine (SMM) from aqueous solution. The performance of SMM adsorption onto ACB[6]-SG at 278, 288, 298, 308, and 318 K and the effects of various solution conditions were evaluated. The adsorption capacity of SMM on ACB[6]-SG increased as the cucurbit[6]uril content of ACB [6]-SG increased. The experimental isotherm data were analyzed using non-linear Freundlich and Henry isotherm equations with five error functions, namely the sum of the squares of the errors, the sum of the absolute errors, the average relative error, the hybrid fractional error function, and Marquardt's percent standard deviation. The error analysis showed that Freundlich model and Henry model described well the SMM adsorption data. Our thermodynamic investigation indicated that the adsorption of SMM onto ACB[6]-SG was a spontaneous and exothermic process. The adsorption was favorable in the pH range of 3.0–4.0. The adsorption affinity of SMM onto ACB[6]-SG increased after adding ions (in the form of NaCl, KCl, CaCl$_2$, or MgCl$_2$), suggesting the predominant role of the hydrophobic force.

Keywords: Sulfa drugs; Water treatment; Cucurbituril; Thermodynamic; Isotherm

1. Introduction

Sulfonamide antibiotics are produced in large quantities and widely used in the farming industry [1]. Sulfonamide antibiotics are refractory compounds; municipal sewage treatment plants cannot effectively eliminate sulfonamides [2]. They could enter surface water and groundwater from wastewater treatment plants and agricultural run-off [3,4]. Investigators in many countries have detected antibiotics in surface water, groundwater, and soil [1,5,6]. In addition, sulfonamides ranked among the most frequently detected pharmaceuticals [5]. Sulfonamide antibiotics are also potentially harmful to aquatic ecosystems, which may eventually reach humans through drinking water and the food chain [7,8]. Thus, adequate treatment of sulfonamide antibiotics is necessary. Adsorbents such as multivalent carbon nanotubes, activated carbon, and microporous materials have been used to remove sulfonamide antibiotics [8–15]. Our team has prepared cucurbituril polymer, and use it to adsorb sulfamonomethoxine (SMM) from aqueous

solution [16]. We also anchored cucurbit[6]uril onto silica gel (ACB[6]-SG), and used it as an adsorbent for SMM [17]. The anchored cucurbituril was prepared by mixing 0.1 g perallyloxyCB[6] (ACB[6]) with 3-Mercaptopropyl-functionalized silica gel (MSG) (5.0 g) under an electrodeless microwave lamp light. The adsorption of SMM onto ACB[6]-SG reached equilibrium in 2 min. The adsorption of SMM onto ACB[6]-SG was studied at 278, 298, and 318 K, and lower temperatures favored higher adsorption efficiencies. The adsorption of SMM on ACB[6]-SG could be well described by both the Henry model and the Freundlich model. But the thermodynamic parameters (the Gibbs free energy (ΔG), heat of adsorption (ΔH), and entropy change (ΔS) of the adsorption were not determined. Moreover, the factors that affect the adsorption of SMM on ACB[6]-SG, such as the ACB[6] content of ACB[6]-SG, pH, and electrolytes in the solution, have not been reported.

In the present study, the Freundlich and Henry isotherms were used to discuss this issue with five error functions. The thermodynamic parameters (the Gibbs free energy (ΔG), heat of adsorption (ΔH), and entropy change (ΔS) of the adsorption were determined. The effects of the ACB[6] content of ACB[6]-SG, pH, and ionic strength on the SMM adsorption were also investigated.

2. Experimental section

2.1. Materials

PerallyloxyCB[6] used in the experiments were synthesized in our laboratory [18,19]. SMM and MSG (200–400 mesh, 1.2 mM/g loading) were purchased from Sigma-Aldrich (USA).

2.2. Preparation of ACB[6]-SG

Dimethylsulfoxide (100 mL) was added to 0.10, 0.50, and 1.00 g of perallyloxyCB[6] (ACB[6]) in separate 500 mL flat-bottom reaction flasks. The perallyloxyCB[6] was completely dissolved by ultrasonication, and then acetone and 0.1 g of benzophenone were added to the solution. The resulting mixture was magnetically stirred. MSG (5.00 g) was combined with the mixture and the resulting suspension was purged with nitrogen for 5 min in darkness. An electrodeless microwave lamp was immersed in the suspension, and was switched on to initiate the reaction, which was carried out for 30 min. The products were subsequently washed with acetone several times in the flask, and then dried in a vacuum oven at 75℃, and

ACB[6]-SG-0.1, ACB[6]-SG-0.5, and ACB[6]-SG-1.0 were obtained.

2.3. Analytical methods

The total nitrogen (TN) was measured according to the method of Kjeldahl nitrogen determination. A mixed catalyst (1.5 g; K_2SO_4:$CuSO_4$·$5H_2O$:Se = 100:10:1) was added to each sample (0.25 g) in a glass digestion tube. A few drops of water and then 5 mL of H_2SO_4 were added to the wet sample. A funnel was used to cover the nozzle of the tube. The wet sample was digested at 360℃ on an electric digestion system for 90 min.

The TN content was calculated as follows:

$$TN = \frac{(V_1 - V_0) \times C \times 0.014}{m} \times 100\% \qquad (1)$$

where TN is the nitrogen content (%); V_1 is the amount of hydrochloric acid standard solution (mL); V_0 is the amount of hydrochloric acid standard solution in the blank sample (mL); C is the concentration of hydrochloric acid standard solution (mol/L); m is the mass of the sample.

The SMM concentration in the solution was measured by high-performance liquid chromatography (HPLC) on a Waters Alliance 2695 separation module equipped with a Waters 2996 photodiode array detector and Millennium[32] software. The chromatographic column used was a Gemini C_{18} (150 mm × 4.6 mm, 5 μm), and the protection column was a Gemini C_{18} (4.0 mm × 3.0 mm i.d.). The mobile phase consisted of HAc–NaAc buffer (0.02 mM L^{-1}, pH 4.75): acetonitrile (80:20). The detection wavelength was 268 nm, the flow rate was 0.8 mL/min, and the column temperature was 30℃.

2.4. Batch adsorption

A series of 0.1000 g of MSG, ACB[6]-SG-0.1, and ACB[6]-SG-0.5 were separately put into 25 mL of SMM solution at concentrations of 0.5–4.0 mg/L at an initial pH of 5.68. All solutions were stored in 40 mL EPA vials equipped with polytetrafluoroethylene-lined screw caps at the 278, 288, 298, 308, and 318 K. The vials were covered with aluminum foil to prevent photodegradation and shaken at 150 rpm for 1 h (1 h is long enough to reach equilibrium [17]). Afterward, the solution was filtered using 2 mL disposable syringes and 0.22 μm filter membranes. The concentration of SMM in the solution was determined by HPLC.

Separate sets of experiments were conducted to test the effects of initial pH and ionic strength. In the pH experiments, the pH of the solution was adjusted with 1.0 mol/L HCl and NaOH. In the ionic-strength experiments, adsorption was performed using a background solution of 0.02, 0.04, 0.08, 0.12, 0.16, and 0.20 mol/L NaCl, KCl, CaCl$_2$, or MgCl$_2$ at pH 5.68 and 298 K.

3. Results and discussion

3.1. Effect of ACB[6] dosage on ACB[6]-SG preparation

Table 1 shows the TN content in the polymer with different dosages of ACB[6]. From Table 1, there was no nitrogen content in the MSG sample, and the TN content in ACB[6]-SG increased as the amount of ACB[6] added increased. This means that the amount of ACB[6] anchored increased with the increasing amount of ACB[6] used. But compared with ACB[6]-SG-0.5, TN amount in ACB[6]-SG-1.0 increased a little. So both ACB[6]-SG-0.1 and ACB[6]-SG-0.5 were used as adsorbents in the following experiments.

3.2. Adsorption of SMM on ACB[6]-SG

The adsorption isotherms of SMM on MSG, ACB[6]-SG-0.1, and ACB[6]-SG-0.5 at various temperatures are presented in Figs. 1–3, respectively. The five isotherms exhibit the same increasing trend in the amounts of adsorbed SMM, and the equilibrium uptake increased linearly with the increase in equilibrium SMM concentration in the range of experimental concentration used. The isotherm shape can provide valuable information on the nature of the solute-surface interaction. The most popular classification of adsorption isotherms (i.e. class S, L, H, C) has been reported by Giles and Smith [20], and the shape of the isotherms indicated C-behavior ("constant partition"). The best-fitted model can be determined based on the use of five error functions to calculate the error deviations between the experimental and predicted equilibrium adsorption data. The sum of the normalized

Table 1
The content of the TN in polymer with different dosages of ACB[6]

Product	TN (%)
MSG	0
ACB[6]-SG-0.1	0.08
ACB[6]-SG-0.5	0.27
ACB[6]-SG-1.0	0.31
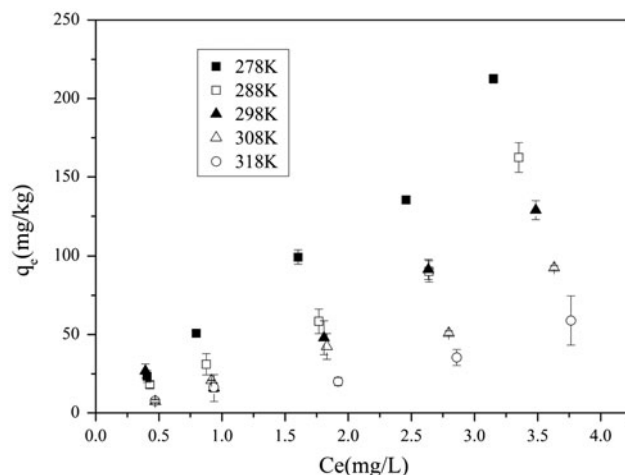
Fig. 1. The adsorption isotherms of SMM on MSG.
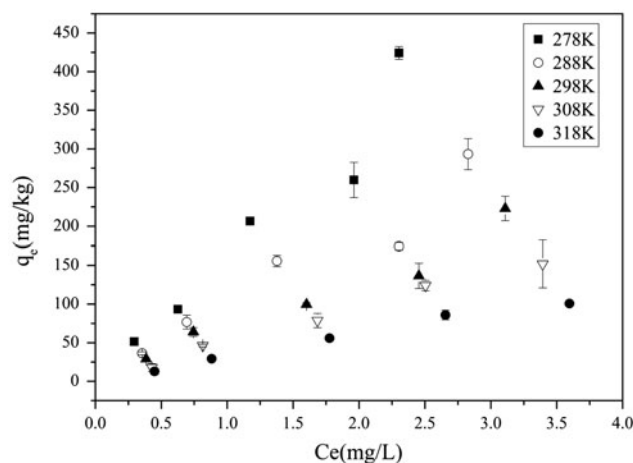
Fig. 2. The adsorption isotherms of SMM on ACB[6]-SG-0.1.

errors (SNE) were used to select the optimum isotherm parameters among the sets of isotherm parameters calculated by the minimization of each of the error functions, and the best fitted parameters for each isotherm model were determined based on the minimum SNE values. The detailed calculation process was described by Foo and Hameed [21].

The Freundlich isotherm is an empirical equation used to describe heterogeneous systems. It can be applied to multilayer adsorption, with non-uniform distributions of adsorption heat and affinities over the heterogeneous surface. The Freundlich isotherm is given by the following [21]:

$$q_e = K_F C_e^{1/n} \tag{2}$$
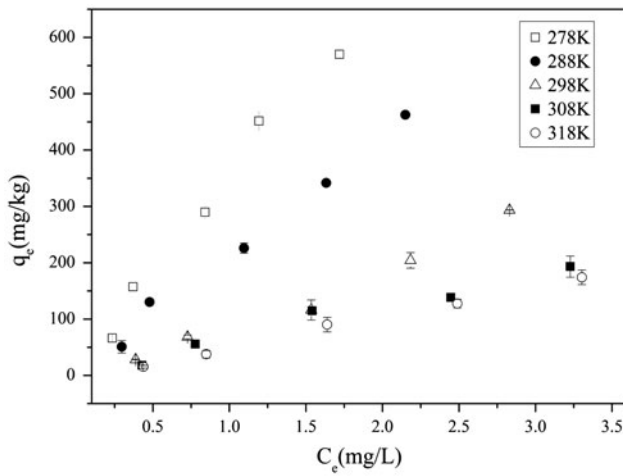
Fig. 3. The adsorption isotherms of SMM on ACB[6]-SG-0.5.

where K_F is the Freundlich constant related to the sorption capacity, and $1/n$ represents the affinity of sorbate to sorbent.

The Henry isotherm, a linear model for partitions, can be described with the following equation:

$$Q_e = K_d C_e \tag{3}$$

where K_d is the Henry parameter (L/g).

The sum of the squares of the errors (SSE) (Eq. (4)): although this is the most common error function in use, isotherm parameters derived using this error function will provide a better fit as the magnitude of the errors and thus the squares of the errors increase-biasing the fit towards the data obtained at the high end of the concentration range.

$$SSE = \sum_{i=1}^{n} (q_{cal} - q_e)_i^2 \tag{4}$$

The sum of the absolute errors (SAE) (Eq. (5)): this is similar to the SSE. The isotherm parameters calculated by this error function will provide a better fit as the magnitude of the errors increase, biasing the fit towards the high concentration data.

$$SAE = \sum_{i=1}^{n} |q_e - q_{cal}|_i \tag{5}$$

The average relative error (ARE) (Eq. (6)): this error function attempts to minimize the fractional error distribution across the entire concentration range.

$$ARE = \frac{\sum |(q_{cal} - q_e)/q_e|}{n} \tag{6}$$

The hybrid fractional error function (HYBRID) was developed by Porter et al. [22] in order to improve the fit of the SSE (Eq. (7)): where p is the number of data points, and n is the number of parameters.

$$HYBRID = \frac{1}{n-p} \sum_{i=1}^{n} \left(\frac{(q_e - q_{cal})^2}{q_e} \right)_i \tag{7}$$

Marquardt's percent standard deviation (MPSD) (Eq. (8)): the error function is similar to a geometric mean error distribution that has been modified to allow for the number of degrees of freedom in the system.

$$MPSD = \sqrt{\frac{1}{n-p} \sum_{i=1}^{n} \left(\frac{q_e - q_{cal}}{q_e} \right)_i^2} \tag{8}$$

where n is the number of experimental data points, q_{cal} is the predicted (calculated) quantity of SMM adsorbed according to the isotherm equations, and q_e is the experimental data.

Gunay reported that nonlinear regression performed better for describing the experimental systems comparing with linear regression analyses [23]. Therefore, the Henry adsorption isotherm and non-linear Freundlich adsorption isotherm were chosen to fit the experimental data. The isotherm parameters were obtained, together with the values of the error measures for each isotherm and the final SNE values as shown in Tables 2–5. In the case of the Freundlich and Henry model, nonlinear regression with error functions reveals differences in the values of isotherm constants. From the Tables 2–5, most of the results suggest that a lower absolute error value was obtained for the Freundlich isotherms at different temperatures. This shows that the Freundlich model exhibited a better fit for the isotherm data. According to the values in Tables 2 and 4, HYBRID provided the best estimation of parameters for the Freundlich models due to it having the lowest SNE values. So the HYBRID error function was selected for evaluating the fitting of the Freundlich isotherm model to experimental data. In addition, higher temperatures lead to smaller values of the adsorption capacity and K_F. Therefore, low temperature is conducive to the adsorption of SMM on ACB[6]-SG. As the value of n of the Freundlich isotherm approaches approximately 1, the isotherm becomes more linear. Thus, ACB[6]-SG could adsorb

Table 2
SNE and error function values for Freundlich isotherm models at different temperatures (adsorbent: ACB[6]-SG-0.1)

Temperature (K)		SSE	SAE	ARE	HYBRID	MPSD
278	K_F	156.4381	156.8934	156.8939	159.6597	158.3256
	n	0.9330	0.8388	1.0957	1.0027	1.0456
	SSE	**6,131.1083**	8,696.5923	9,416.1781	6,506.6834	7,566.0203
	SAE	135.3579	**125.4621**	152.6243	140.3859	146.4884
	ARE	0.1267	0.1511	**0.1086**	0.1174	0.1133
	HYBRID	7.5942	12.4325	8.6013	**7.0383**	7.4159
	MPSD	0.1912	0.2665	0.1643	0.1637	**0.1587**
	SNE	3.7048	4.7456	4.0271	**3.5682**	3.7051
288	K_F	101.7742	108.7434	108.7434	101.2452	98.8479
	n	1.0823	1.0478	1.0478	1.1131	1.1051
	SSE	**3,210.9195**	4,537.8922	4,537.8922	3,316.3201	3,491.3637
	SAE	98.6027	**78.8438**	78.8394	103.5102	107.5892
	ARE	0.1205	0.1091	**0.1091**	0.1257	0.1263
	HYBRID	5.7345	8.8096	8.8096	**5.5086**	5.6776
	MPSD	0.1827	0.2321	0.2321	0.1793	**0.1767**
	SNE	**4.0163**	4.5967	4.5967	4.0239	4.1752
298	K_F	65.0699	65.1079	66.2619	70.0843	70.1357
	n	0.9888	0.9216	1.1570	1.1085	1.1440
	SSE	**1,236.8936**	1,694.4298	2,361.2441	1,389.3862	1,594.4534
	SAE	68.1362	**67.7288**	66.5225	67.5769	68.7870
	ARE	0.1418	0.1642	**0.0923**	0.1077	0.1090
	HYBRID	3.5930	5.3115	4.1863	**3.0089**	3.1172
	MPSD	0.2040	0.2507	0.1690	0.1550	**0.1520**
	SNE	3.8681	4.7022	3.9915	**3.4114**	3.5322
308	K_F	50.8990	50.8787	44.5153	48.3018	46.3347
	n	1.0963	1.1177	0.9160	1.0328	0.9734
	SSE	**112.8634**	128.4759	415.1310	135.4941	219.9983
	SAE	22.8429	**20.8551**	30.5242	23.9778	26.7361
	ARE	0.1065	0.1065	**0.0731**	0.0913	0.0810
	HYBRID	0.9410	1.0430	1.4844	**0.7610**	0.9274
	MPSD	0.2016	0.2123	0.1487	0.1494	**0.1316**
	SNE	3.5957	3.6880	4.3761	**3.1771**	3.4017
318	K_F	33.4528	33.3736	30.4598	31.5148	30.4598
	n	1.1221	1.1582	0.9468	1.0505	1.0012
	SSE	**64.6067**	86.5253	293.8287	77.5966	110.0340
	SAE	14.2017	**14.0045**	20.1873	16.4217	18.7474
	ARE	0.0816	0.0882	**0.0556**	0.0682	0.0646
	HYBRID	0.5203	0.6704	1.0260	**0.3736**	0.4486
	MPSD	0.1658	0.1832	0.1099	0.1026	**0.0869**
	SNE	3.2607	3.6416	4.2303	**2.7750**	2.9472

Note: Values in bold represent minimum error values and minimum sum of normalized errors (SNE).

SMM through hydrophobic interactions. For the adsorption of SMM onto MSG, values of parameters calculated for all temperatures studied using the HYBRID function are also shown in Table 6. Since equilibrium data were characterized by the Freundlich isotherm model, the thermodynamic parameters, such as enthalpy change (ΔH), Gibbs free energy change (ΔG), and entropy change (ΔS), can be estimated with the following Gibbs free energy equations [24]:

$$\Delta G = -RT \ln K_F \tag{9}$$

Table 3
SNE and error function values for Henry isotherm models at different temperatures (adsorbent: ACB[6]-SG-0.1)

Temperature (K)		SSE	SAE	ARE	HYBRID	MPSD	SSE
278	k_H	163.7461	175.9520	174.5842	159.4745	158.1638	
	SSE	**6,286.2547**	7,926.2006	7,579.2432	6,487.1128	6,629.2835	
	SAE	135.2432	**121.6003**	122.4140	140.2997	141.8511	
	ARE	0.1156	0.1124	**0.1100**	0.1178	0.1185	
	HYBRID	7.2815	10.6478	10.0735	**7.0390**	7.0618	
	MPSD	0.1700	0.2182	0.2110	0.1642	**0.1639**	
	SNE	**4.1850**	4.8058	4.6605	4.2152	4.2507	
288	k_H	95.6224	103.7061	103.7061	94.9204	96.6300	
	SSE	**3,316.5765**	4,348.9975	4,348.9975	3,324.3620	3,332.6184	
	SAE	105.5776	**82.4708**	**82.4708**	107.6481	102.6055	
	ARE	0.1398	**0.1050**	**0.1050**	0.1432	0.1350	
	HYBRID	6.3761	8.4109	8.4109	**6.3631**	6.4406	
	MPSD	0.2017	0.2219	0.2219	0.2026	**0.2013**	
	SNE	4.3867	4.4994	4.4994	4.4340	**4.3351**	
298	k_H	65.7441	71.7010	71.010	65.3009	67.0345	
	SSE	**1,237.9501**	1,910.4494	1,910.4494	1,241.6722	1,269.5118	
	SAE	68.0085	**66.9332**	**66.9332**	68.0885	67.7755	
	ARE	0.1376	**0.1320**	**0.1320**	0.1380	0.1364	
	HYBRID	3.4882	5.2137	5.2137	**3.4798**	3.6071	
	MPSD	0.1966	0.2143	0.2143	0.1978	**0.1950**	
	SNE	**4.2303**	4.9396	4.9396	4.2404	4.2501	
308	k_H	46.7286	46.6922	46.6921	47.1255	46.7171	
	SSE	**166.6063**	166.6348	166.6349	169.9887	166.6091	
	SAE	24.3301	**24.2504**	**24.2504**	25.1987	24.3049	
	ARE	0.0825	0.0823	**0.0823**	0.0849	0.0824	
	HYBRID	0.8190	0.8209	0.8209	**0.8091**	0.8195	
	MPSD	0.1347	0.1347	0.1347	0.1352	**0.1347**	
	SNE	4.9114	**4.9083**	**4.9083**	4.9856	4.9098	
318	k_H	29.9072	31.4585	31.4585	30.2708	30.4463	
	SSE	**104.4305**	162.4946	162.4946	107.6193	111.4429	
	SAE	19.4752	**17.5049**	**17.5049**	19.0135	18.7905	
	ARE	0.0669	0.0600	**0.0600**	0.0653	0.0645	
	HYBRID	0.4632	0.5950	0.5950	**0.4496**	0.4528	
	MPSD	0.0898	0.0969	0.0969	0.0872	**0.0869**	
	SNE	4.3479	4.7957	4.7957	**4.2701**	4.2726	

Note: Values in bold represent minimum error values and minimum sum of normalized errors (SNE).

$$\Delta G = \Delta H - T\Delta S \tag{10}$$

then:

$$\ln K_F = -\Delta H/RT + \Delta S/R \tag{11}$$

where ΔG (kJ/mol) is the free energy of adsorption; ΔH (kJ/mol) is the apparent enthalpy of adsorption; ΔS (J/K mol) is the entropy of adsorption; R is the universal gas constant (8.314 J/mol K); T is the absolute temperature (K); and K_F is the standard thermodynamic equilibrium constant defined by the Freundlich model $[(mg/g)/(mg/L)^n]$. Values of ΔH and ΔS can be determined from the slope and the intercept of the plot between $\ln K_F$ vs. $1/T$.

The predicted thermodynamic constants (ΔG, ΔH, and ΔS) shown in Table 7 can be determined through linearization of the test data, as shown in Fig. 4. The values of ΔG are negative at all temperatures and the degree of spontaneity of the adsorption decreases with

Table 4
SNE and error function values for Freundlich isotherm models at different temperatures (adsorbent: ACB[6]-SG-0.5)

Temperature (K)		SSE	SAE	ARE	HYBRID	MPSD
278	K_F	357.1473	355.7798	355.7580	348.1267	349.2519
	n	1.0799	1.0888	1.1502	0.8729	1.0104
	SSE	**2,505.8239**	2,875.3584	8,829.2971	3,032.4132	4,747.4451
	SAE	104.7817	**95.3891**	152.9707	111.3573	125.2658
	ARE	0.1323	0.1421	**0.0996**	0.1141	0.1033
	HYBRID	5.5169	7.4995	8.5064	**4.3764**	5.2645
	MPSD	0.2540	0.3095	0.1890	0.1862	**0.1653**
	SNE	3.3691	3.8309	4.3116	**2.9905**	3.2365
288	K_F	215.1843	215.4941	205.0384	203.9399	212.2478
	n	1.0108	1.0204	0.9410	0.9348	0.9942
	SSE	**1,048.7758**	1,388.0584	1,388.0584	1,083.4706	1,403.9182
	SAE	62.7342	**45.4314**	45.4314	47.2974	60.3495
	ARE	0.1114	0.0792	**0.0792**	0.1010	0.0898
	HYBRID	3.2712	3.6432	3.6432	**3.1625**	3.5355
	MPSD	0.2015	0.1735	0.1735	0.1847	**0.1723**
	SNE	4.6449	4.2849	4.2849	**4.2169**	4.5936
298	K_F	76.6551	76.6551	76.6778	82.6153	83.7768
	n	0.7864	0.7748	0.7969	0.8566	0.8942
	SSE	**619.5982**	663.5123	651.3161	765.9582	1,115.4156
	SAE	46.9040	**46.0471**	47.6025	48.9225	58.4724
	ARE	0.1221	0.1269	**0.1177**	0.0864	0.0870
	HYBRID	2.5586	2.7725	2.4608	**2.0602**	2.2583
	MPSD	0.1986	0.2076	0.1913	0.1430	**0.1358**
	SNE	4.1993	4.3824	4.1346	**3.6361**	4.1543
308	K_F	67.2019	67.2021	67.2021	59.8514	54.5287
	n	1.1203	1.1098	1.1098	0.9829	0.8766
	SSE	**564.9328**	587.0806	587.0806	739.7963	1,246.035
	SAE	44.3843	**41.8717**	41.8717	52.8333	70.3187
	ARE	0.2059	0.2135	**0.2135**	0.1737	0.1631
	HYBRID	4.5401	5.2978	5.2978	**3.2168**	4.1013
	MPSD	0.4521	0.5015	0.5015	0.2844	**0.2309**
	SNE	3.8074	4.0666	4.0666	**3.3329**	3.9985
318	K_F	48.6312	48.8040	46.9033	41.9724	45.7251
	n	0.9325	0.9350	0.9107	0.8282	0.8775
	SSE	**92.5372**	105.8684	220.7152	125.8093	225.5586
	SAE	18.1137	**14.5113**	22.2950	18.3757	26.3304
	ARE	0.0981	0.0736	**0.0541**	0.0610	0.0601
	HYBRID	0.7831	0.6146	0.8337	**0.5289**	0.6798
	MPSD	0.1882	0.1443	0.1022	0.1098	**0.0877**
	SNE	4.0375	3.2747	3.9198	**3.0953**	3.8940

Note: Values in bold represent minimum error values and minimum sum of normalized errors (SNE).

increasing temperature. Negative values of ΔG show the spontaneous nature of the sorption processes. The negative value for ΔH indicates that the adsorption was an exothermic process, which is supported by the decreasing adsorption of SMM with increase in temperature. The negative value of ΔS indicated a greater stability of the adsorption process and the adsorbed

SMM is in a stable arrangement and a more ordered form [25]. This indicates increased randomness at the solid–liquid interface during the sorption process and also indicated that the process is entropy driven and not enthalpy driven [26]. Bonding strengths typical of physisorption bonds are of <84 kJ/mol, and chemisorption bond strengths can range from 84 to

Table 5
SNE and error function values for Henry isotherm models at different temperatures (adsorbent: ACB[6]-SG-0.5)

Temperature (K)		SSE	SAE	ARE	HYBRID	MPSD	SSE
278	k_H	350.2069	347.6951	344.2196	344.2196	349.0051	
	SSE	**3,188.0968**	3,251.9132	3,251.9132	3,197.1648	3,568.2095	
	SAE	111.5956	**107.3129**	107.3129	113.2102	109.5683	
	ARE	0.1112	0.1081	**0.1081**	0.1124	0.1094	
	HYBRID	4.4030	4.4912	4.4912	**4.3958**	4.7952	
	MPSD	0.1796	0.1778	0.1778	0.1806	**0.1768**	
	SNE	4.7812	**4.7421**	**4.7421**	4.8127	4.9201	
288	k_H	213.9716	213.2251	209.3626	209.3626	212.6509	
	SSE	**1,069.1050**	1,200.4818	1,200.4818	1,072.0080	1,500.1734	
	SAE	58.6244	**57.0933**	57.0933	58.3968	66.0848	
	ARE	0.1037	0.0982	**0.0982**	0.1028	0.0997	
	HYBRID	3.1699	3.2628	3.2628	**3.1670**	3.5325	
	MPSD	0.1882	0.1842	0.1842	0.1874	**0.1832**	
	SNE	4.4971	4.5135	4.5135	**4.4818**	4.9349	
298	k_H	95.7276	95.8573	93.5554	93.5554	91.2778	
	SSE	**1,558.7043**	1,642.4787	1,642.4789	1,890.2728	3,496.3008	
	SAE	68.4841	**64.3918**	64.3918	73.0874	97.8688	
	ARE	0.1401	0.1238	**0.1238**	0.1257	0.1310	
	HYBRID	4.2844	3.8428	3.8428	**3.6976**	4.8765	
	MPSD	0.2420	0.2195	0.2195	0.2006	**0.1751**	
	SNE	4.0242	**3.7064**	**3.7064**	3.7718	4.6586	
308	k_H	60.5644	60.8303	59.8478	59.8478	60.6019	
	SSE	**696.4451**	715.3274	715.3274	697.4656	1,227.7882	
	SAE	51.14256	**47.4250**	47.4250	50.2783	63.6148	
	ARE	0.1770	0.1709	**0.1709**	0.1756	0.1800	
	HYBRID	3.2391	3.2630	3.2630	**3.2367**	4.3868	
	MPSD	0.3019	0.2939	0.2939	0.2999	**0.2778**	
	SNE	4.0929	**3.9949**	**3.9949**	4.0652	4.9202	
318	k_H	52.1607	52.7355	51.3006	50.5702	45.2183	
	SSE	**128.0778**	134.9191	143.3941	180.4594	1,126.0479	
	SAE	22.7288	**22.0587**	23.7315	28.2197	61.1029	
	ARE	0.1458	0.1496	**0.1401**	0.1410	0.1472	
	HYBRID	1.6464	1.7704	1.5317	**1.5010**	3.1470	
	MPSD	0.2937	0.3047	0.2782	0.2660	**0.2193**	
	SNE	2.9474	3.0433	**2.8520**	2.9146	4.7037	

Note: Values in bold represent minimum error values and minimum sum of normalized errors (SNE).

Table 6
Parameters and error values for Freundlich model at different temperatures (adsorbent: MSG)

	278 K	288 K	298 K	308 K	318 K
K_F	59.9154	34.1936	22.9968	19.4711	13.5518
n	0.9651	0.8655	0.7303	0.8888	1.0072
R^2	0.9926	0.9916	0.9960	0.9983	0.9992
HYBRID	1.1859	2.8377	5.9252	1.4387	1.4063

420 kJ/mol [27]. Therefore, binding of SMM on ACB [6]-SG and MSG is physisorption. Additionally, entropy and enthalpy changes for hydrophobic adsorption have negative values [28].

To confirm whether the adsorption mechanism occurs via hydrophobic interaction, we performed adsorption experiments using ethanol in place of water as the solvent. The result showed that there was no adsorption of SMM on ACB[6]-SG in ethanol. The ethyl group in ethanol would inhibit the hydrophobic

Table 7
The thermodynamic properties of the adsorption of SMM on MSG, ACB[6]-SG-0.1, and ACB[6]-SG-0.5

Adsorbent	Temperature (K)	Enthalpy (ΔH) (kJ/mol)	Entropy (ΔS) (J/K mol)	Free energy change (ΔG) (kJ/mol)
MSG	278	−26.6603	−62.4348	−9.2898
	288			−8.0167
	298			−7.1164
	308			−6.7386
	318			−5.9161
ACB[6]-SG-0.1	278	−29.9739	−62.3688	−11.5144
	288			−10.4805
	298			−9.6456
	308			−8.8008
	318			−7.8316
ACB[6]-SG-0.5	278	−41.2698	−99.7589	−13.2910
	288			−12.0700
	298			−10.0190
	308			−9.2874
	318			−8.4820
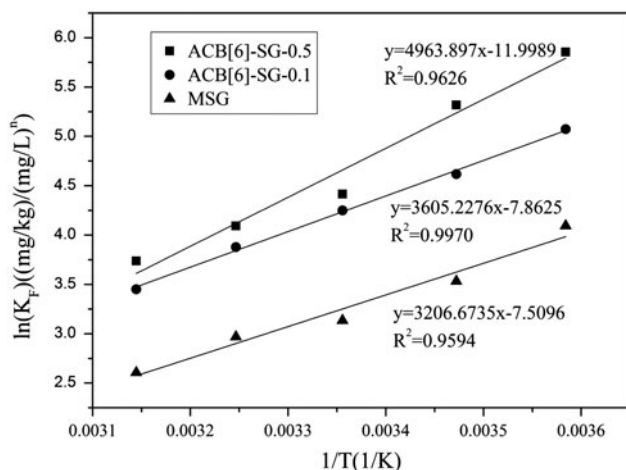
Fig. 4. Plots of $\ln K_F$ vs. $1/T$ for adsorption of SMM on ACB[6]-SG and MSG.

interaction between ACB[6]-SG and SMM [29], and thereby hinder adsorption in ethanol. Hence, the adsorption of SMM on ACB[6]-SG was hypothesized to occur mainly through hydrophobic interactions.

3.3. Effect of pH

Fig. 5 showed the pH dependence of SMM adsorption on ACB[6]-SG at initial SMM concentrations of 4.0 mg/L at 298 K at initial pH 2.0–12.0. As shown in Fig. 5, solution pH was a key parameter that affected the adsorption of SMM onto ACB[6]-SG.

SMM adsorption onto ACB[6]-SG initially increased with increase in pH from 2.0 to 4.0, and then decreased with further increase in pH from 4.0 to 12.0. Adsorption of solute from aqueous phase is generally influenced by the characteristics of both adsorbate and adsorbent. SMM possesses an amine group ($-NH_2-$) with pK_{a1} of 2 and a sulfonamide group ($-SO_2-NH-$) with pK_{a2} of 6.0 [30,31]. SMM is amphoteric in solution, and can exist in the dissociated or undissociated forms under different pH conditions. So SMM can be cationic, neutral, or anionic depending on the solution pH.
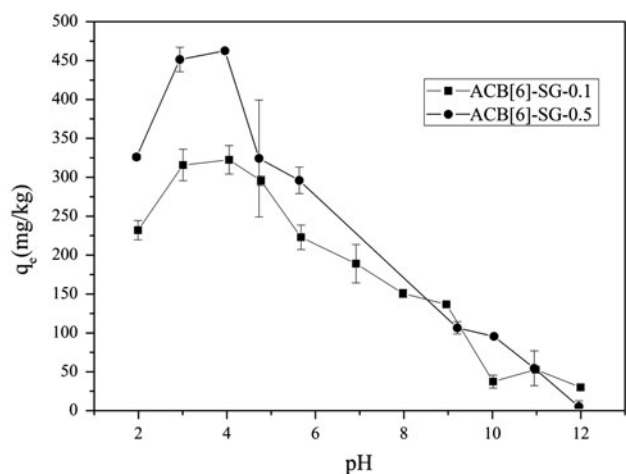
Fig. 5. Effect of pH on the equilibrium adsorption (q_e) for the adsorption of SMM on ACB[6]-SG (initial SMM concentration, 4 mg/L; agitation speed, 150 rpm; contact time, 60 min; temperature, 298 K).

In Fig. 5, high adsorption efficiencies were achieved at pH values between pK_{a1} and pK_{a2}, where almost SMM molecules exist in the neutral form, indicating that neutral SMM is easily adsorbed onto ACB[6]-SG compared to those in the cationic or anionic form. The results suggests that the dominant adsorption mechanism was based on hydrophobic interactions between SMM and ACB[6]-SG.

Fig. 6 showed adsorption isotherms of SMM on ACB[6]-SG at pH 2.0 and 3.5, clearly revealing that, at various initial concentrations of SMM, the adsorption capacity was greater at pH 3.5 than at pH 2.0. The adsorption isotherms are highly linear over the concentration range examined, indicating that SMM did not saturate available adsorption sites. However, solubility limitations prevented investigation of saturation of SMM adsorption.

3.4. Effect of electrolyte

Fig. 7 depicts the effects of ionic strength on the adsorption of SMM on ACB[6]-SG-0.1. The figure shows that the adsorption capacity increased significantly when electrolyte was used in the experiment. At the same time, the adsorption capacity did not significantly change with the cationic ions concentration increasing. In the experiment, the electrolyte concentration was three orders of magnitude of the SMM concentration. The introduction of Na^+, K^+, Ca^{2+}, or Mg^{2+}, which are strongly hydrated, reduces the number of water molecules around the SMM polar group
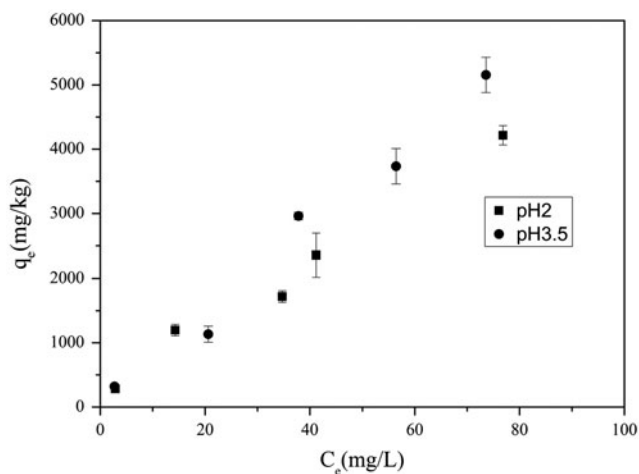
Fig. 7. Effect of ionic strength (NaCl, KCl, MgCl$_2$, or CaCl$_2$) on the equilibrium adsorption (q_e) of SMM on ACB[6]-SG-0.1 (SMM initial concentration, 4 mg/L; agitation speed, 150 rpm; contact time, 60 min; pH 5.68).

or charged group, and thereby weakens the SMM hydrophilicity as it enhances the hydrophobic effect [23,32]. Thus, binding of SMM to the hydrophobic surface of ACB[6]-SG becomes more likely. The results manifest that hydrophobic interaction was the main force behind the adsorption. As the concentration of Na^+ (K^+, Ca^{2+}, and Mg^{2+}) is already three orders of magnitude of the SMM concentration, adding additional amounts of Na^+, K^+, Ca^{2+}, or Mg^{2+} did not promote the adsorption.

4. Conclusions

The solubility of cucurbituril increases in acid solution and in the presence of salts (such as Ca^{2+}, Na^+, and K^+) [33], which limits their potential use as an environmental adsorbent. This study indicates that anchored cucurbut[6]urils are effective adsorbents for sulfonamide antibiotics, such as SMM, in water treatments. The influence of temperature on adsorption is significant; in particular, low temperature is conducive to adsorption. Comparing with the Henry isotherm, the non-linear Freundlich model performed better a little for the equilibrium data. The adsorption is an exothermic process, and negative values of entropy and enthalpy changes verified this adsorption of SMM on ACB[6]-SG via hydrophobic adsorption. Additionally, the observed effects of pH on adsorption show that the adsorption of SMM on ACB[6]-SG is favorable at about pH 3.0–4.0. Adding ions (in the form of NaCl, KCl, CaCl$_2$, or MgCl$_2$) to the solution significantly strengthens the adsorption, but varying the ionic

Fig. 6. Adsorption isotherms of SMM plotted as equilibrium adsorption (q_e) vs. concentration of SMM in solution (C_e) at the adsorption equilibrium with ACB[6]-SG. Adsorption isotherms on a linear scale are shown (agitation speed, 150 rpm; contact time, 60 min; temperature, 298 K).

strength from 0.02 to 0.20 mol/L salt does not significantly change the adsorption capacity. Findings in this study show promise in the use of cucurbituril-anchored carriers as adsorbents for the removal of sulfonamide antibiotics from aqueous solution.

Acknowledgment

References

[1] A.K. Sarmah, M.T. Meyer, A.B.A. Boxall, A global perspective on the use, sales, exposure pathways, occurrence, fate and effects of veterinary antibiotics (VAs) in the environment, Chemosphere 65 (2006) 725–759.

[2] T.A. Ternes, A. Joss, H. Siegrist, Peer reviewed: Scrutinizing pharmaceuticals and personal care products in wastewater treatment, Environ. Sci. Technol. 38 (2004) 392A–399A.

[3] S.C. Kim, K. Carlson, Quantification of human and veterinary antibiotics in water and sediment using SPE/LC/MS/MS, Anal. Bioanal. Chem. 387 (2007) 1301–1315.

[4] K. Stoob, H.P. Singer, S.R. Mueller, R.P. Schwarzenbach, C.H. Stamm, Dissipation and transport of veterinary sulfonamide antibiotics after manure application to grassland in a small catchment, Environ. Sci. Technol. 41 (2007) 7349–7355.

[5] D.W. Kolpin, E.T. Furlong, M.T. Meyer, E.M. Thurman, S.D. Zaugg, L.B. Barber, H.T. Buxton, Pharmaceuticals, hormones, and other organic wastewater contaminants in U.S. streams, 1999–2000: A national reconnaissance, Environ. Sci. Technol. 36 (2002) 1202–1211.

[6] N. Watanabe, B.A. Bergamaschi, K.A. Loftin, M.T. Meyer, T. Harter, Use and environmental occurrence of antibiotics in freestall dairy farms with manured forage fields, Environ. Sci. Technol. 44 (2010) 6591–6600.

[7] R. Hirsch, T. Ternes, K. Haberer, K.L. Kratz, Occurrence of antibiotics in the aquatic environment, Sci. Total Environ. 225 (1999) 109–118.

[8] D. Zhang, B. Pan, H. Zhang, P. Ning, B. Xing, Contribution of different sulfamethoxazole species to their overall adsorption on functionalized carbon nanotubes, Environ. Sci. Technol. 44 (2010) 3806–3811.

[9] L. Ji, W. Chen, S. Zheng, Z. Xu, D. Zhu, Adsorption of sulfonamide antibiotics to multiwalled carbon nanotubes, Langmuir 25 (2009) 11608–11613.

[10] F. Ogata, H. Tominaga, M. Kangawa, K. Inoue, N. Kawasaki, Removal of sulfa drugs by sewage treatment in aqueous solution systems: Activated carbon treatment and ozone oxidation, J. Oleo Sci. 61 (2012) 217–225.

[11] I. Braschi, S. Blasioli, L. Gigli, C.E. Gessa, A. Alberti, A. Martucci, Removal of sulfonamide antibiotics from water: Evidence of adsorption into an organophilic zeolite Y by its structural modifications, J. Hazard. Mater. 178 (2010) 218–225.

[12] I. Braschi, G. Gatti, G. Paul, C.E. Gessa, M. Cossi, L. Marchese, Sulfonamide antibiotics embedded in high silica zeolite Y: A combined experimental and theoretical study of host–guest and guest–guest interactions, Langmuir 26 (2010) 9524–9532.

[13] I. Braschi, G. Paul, G. Gatti, M. Cossi, L. Marchese, Embedding monomers and dimers of sulfonamide antibiotics into high silica zeolite Y: An experimental and computational study of the tautomeric forms involved, RSC Adv. 3 (2013) 7427–7437.

[14] A. Martucci, M.A. Cremonini, S. Blasioli, L. Gigli, G. Gatti, L. Marchese, I. Braschi, Adsorption and reaction of sulfachloropyridazine sulfonamide antibiotic on a high silica mordenite: A structural and spectroscopic combined study, Microporous Mesoporous Mater. 170 (2013) 274–286.

[15] S. Blasioli, A. Martucci, G. Paul, L. Gigli, M. Cossi, C.T. Johnston, L. Marchese, I. Braschi, Removal of sulfamethoxazole sulfonamide antibiotic from water by high silica zeolites: A study of the involved host–guest interactions by a combined structural, spectroscopic, and computational approach, J. Colloid Interface Sci. 419 (2014) 148–159.

[16] H.T. Qiao, Y. Liu, Y.H. Dong, S.R. Li, P. Wang, T. Jin, Adsorption of sulfamonomethoxine antibiotics to cucurbit[6]uril polymer: Kinetics and thermodynamic studies, Desalin. Water Treat. (in press), doi:10.1080/19443994.2013.878255.

[17] T. Jin, D.Q. Chen, Y. Liu, Y.H. Dong, H.T. Qiao, X.L. Chen, Preparation of cucurbit[6]uril anchored silica gel and its adsorption characteristics of sulfamonomethoxine, Acta Sci. Circumst. 33 (2013) 991–996 (in Chinese).

[18] A. Day, A.P. Arnold, R.J. Blanch, B. Snushall, Controlling factors in the synthesis of cucurbituril and its homologues, J. Org. Chem. 66 (2001) 8094–8100.

[19] S.Y. Jon, N. Selvapalam, D.H. Oh, J.K. Kang, S.Y. Kim, Y.J. Jeon, J.W. Lee, K. Kim, Facile synthesis of cucurbit[n]uril derivatives via direct functionalization: Expanding utilization of cucurbit[n]uril, J. Am. Chem. Soc. 125 (2003) 10186–10187.

[20] C.H. Giles, D. Smith, A general treatment and classification of the solute adsorption isotherm. I. Theoretical, J. Colloid Interface Sci. 47 (1974) 755–765.

[21] K.Y. Foo, B.H. Hameed, Insights into the modeling of adsorption isotherm systems, Chem. Eng. J. 156 (2010) 2–10.

[22] J.F. Porter, G. McKay, K.H. Choy, The prediction of sorption from a binary mixture of acidic dyes using single- and mixed-isotherm variants of the ideal adsorbed solute theory, Chem. Eng. Sci. 54 (1999) 5863–5885.

[23] A. Gunay, Application of nonlinear regression analysis for ammonium exchange by natural (Bigadiç) clinoptilolite, J. Hazard. Mater. 148 (2007) 708–713.

[24] D. Kavitha, C. Namasivayam, Experimental and kinetic studies on methylene blue adsorption by coir pith carbon, Bioresour. Technol. 98 (2007) 14–21.

[25] D. Xu, X.L. Tan, X.K. Chen, X.K. Wang, Adsorption of Pb(II) from aqueous solution to MX-80 bentonite: Effect of pH, ionic strength, foreign ions and temperature, Appl. Clay Sci. 41 (2008) 37–46.

[26] Y. Shih, Y. Su, R. Ho, P. Su, C. Yang, Distinctive sorption mechanisms of 4-chlorophenol with black carbons as elucidated by different pH, Sci. Total Environ. 433 (2012) 523–529.

[27] Y.S. Aldegs, M.I. Elbarghouthi, A.H. Elsheikh, G.M. Walker, Effect of solution pH, ionic strength, and temperature on adsorption behavior of reactive dyes on activated carbon, Dyes Pigm. 77 (2008) 16–23.

[28] B.K. Głód, P.W. Alexander, Z.L. Chen, P.R. Haddad, Thermodynamic investigation of sample retention mechanism in ion-exclusion chromatography with inclusion compound in the mobile phase, Anal. Chim. Acta 306 (1995) 267–272.

[29] J.Z. Li, K.D. Yao, Adsorption from aqueous solution based on the synergism between hydrogen bonding and hydrophobic interactions, J. Appl. Polym. Sci. 96 (2005) 841–845.

[30] T. Li, Z.G. Shi, M.M. Zheng, Y.Q. Feng, Multiresidue determination of sulfonamides in chicken meat by polymer monolith microextraction and capillary zone electrophoresis with field-amplified sample stacking, J. Chromatogr. A 1205 (2008) 163–170.

[31] C.E. Lin, C.C. Chang, W.C. Lin, Migration behavior and separation of sulfonamides in capillary zone electrophoresis III. Citrate buffer as a background electrolyte, J. Chromatogr. A 768 (1997) 105–112.

[32] T. Sennerfors, D. Solberg, F. Tiberg, Adsorption of polyelectrolyte–nanoparticle systems on silica: Influence of ionic strength, J. Colloid Interface Sci. 254 (2002) 222–226.

[33] S. Karcher, A. Kornmüller, M. Jekel, Cucurbituril for water treatment. Part I: Solubility of cucurbituril and sorption of reaction dyes, Water Res. 35 (2001) 3309–3316.